

UCLA

UCLA Previously Published Works

Title

Transcriptional Evaluation of the Ductus Arteriosus at the Single-Cell Level Uncovers a Requirement for Vim (Vimentin) for Complete Closure

Permalink

<https://escholarship.org/uc/item/25q9r3b7>

Journal

Arteriosclerosis Thrombosis and Vascular Biology, 42(6)

ISSN

1079-5642

Authors

Salvador, Jocelynda
Hernandez, Gloria E
Ma, Feiyang
[et al.](#)

Publication Date

2022-06-01

DOI

10.1161/atvbaha.121.317172

Peer reviewed



HHS Public Access

Author manuscript

Arterioscler Thromb Vasc Biol. Author manuscript; available in PMC 2023 June 01.

Published in final edited form as:

Arterioscler Thromb Vasc Biol. 2022 June ; 42(6): 732–742. doi:10.1161/ATVBAHA.121.317172.

Transcriptional evaluation of the ductus arteriosus at the single-cell level uncovers a requirement for vimentin for complete closure

Jocelynda Salvador^{&,1}, Gloria E. Hernandez^{&,2}, Feiyang Ma², Cyrus W. Abrahamson¹, Matteo Pellegrini³, Robert Goldman¹, Karen M. Ridge^{1,4}, M. Luisa Iruela-Arispe^{1,*}

¹Department of Cell and Development Biology, Feinberg School of Medicine, Northwestern University, Chicago, IL 60611, USA

²Molecular Biology Institute, University of California, Los Angeles, Los Angeles, CA 90095, USA.

³Department of Molecular, Cell and Development Biology, University of California, Los Angeles, Los Angeles, CA 90095, USA.

⁴Department of Medicine, Feinberg School of Medicine, Northwestern University, Chicago, IL 60611, USA.

Abstract

BACKGROUND: Failure to close the ductus arteriosus, patent ductus arteriosus (PDA), accounts for 10% of all congenital heart defects. Despite significant advances in PDA management, including pharmacological treatment targeting the prostaglandin pathway, a proportion of patients fail to respond and must undergo surgical intervention. Thus, further refinement of the cellular and molecular mechanisms that govern vascular remodeling of this vessel is required.

APPROACH: We performed single cell RNAseq of the ductus arteriosus in mouse embryos at E18.5, and neonatal stages P0.5, and P5 to identify transcriptional alterations that might be associated with remodeling.

RESULTS: The intermediate filament vimentin emerged as a candidate that might contribute to closure of the ductus arteriosus. Indeed, mice with genetic deletion of vimentin fail to complete vascular remodeling of the ductus arteriosus. To seek mechanisms, we turned to the RNAseq data that indicated changes in *Jagged1* with similar profile to vimentin and pointing to potential links

*Please address correspondence to: M. Luisa Iruela-Arispe, Ph.D., 303 E. Superior st. SQ 8-522, Northwestern University, Chicago, IL 60611, arispe@northwestern.edu - Phone: 312-503-7958.

[&]Both contributed equally to this work

CONTRIBUTIONS

JC and GEH designed and performed experiments, wrote and edited the manuscript.

FM performed bioinformatic analysis of scRNAseq data.

CWA performed experiments.

KMR provided the vimentin KO mouse and intellectual input.

RG and **MP** provided intellectual discussion.

MLIA conceived the study, designed the experiments, wrote and edited the manuscript.

All authors discussed the results and had the opportunity to comment on the manuscript.

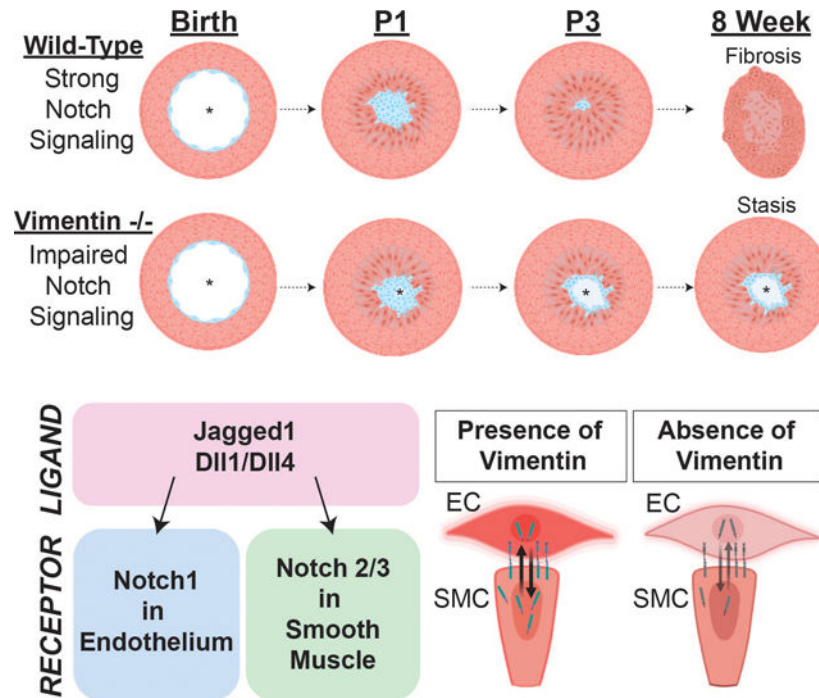
DISCLOSURES

The authors have nothing to disclose.

with Notch. In fact, Notch3 signaling was impaired in vimentin null mice and vimentin null mice phenocopies PDA in Jagged1 endothelial and smooth muscle deleted mice.

CONCLUSIONS: Through single-cell RNA-sequencing and by tracking closure of the ductus arteriosus in mice, we uncovered the unexpected contribution of vimentin in driving complete closure of the ductus arteriosus through a mechanism that includes deregulation of the Notch signaling pathway.

Graphical Abstract



Keywords

endothelium; smooth muscle cells; single-cell RNA-seq; vascular remodelling

INTRODUCTION

During fetal life, the ductus arteriosus, or ductus Botalli, is the vessel that connects the left pulmonary artery to the descending aorta. This structure is critical during fetal development as it diverts the blood emanating from the right ventricle away from the high-resistance pulmonary circulation and into the systemic circulation. At birth a combination of physical and biochemical changes including: the inflation of the lungs, the resulting changes in hemodynamics and alterations in prostaglandin levels trigger the closure of the ductus arteriosus. This essential physiological event prevents the mixture of non-oxygenated blood (from the pulmonary artery) with oxygenated blood (from the aorta).

Abnormal persistence of this vessel, a condition termed patent ductus arteriosus (PDA), frequently occurs in pre-term infants and it is associated with subsequent mortality (1–

3). Clinical management of PDA ranges from surgical ligation to pharmacotherapy with cyclooxygenase inhibitors (1–3). Unfortunately, a percentage of patients with PDA fail to respond to these inhibitors. Consequently, a more refined understanding of the processes involved in closure of the ductus arteriosus could offer novel targets for intervention and improved therapies.

At the cellular level, the postnatal closure of the ductus arteriosus is thought to involve the contribution of smooth muscle cells, endothelial cells, and fibroblasts leading to the eventual transformation of this embryonic vessel into a ligament (1–3). Initially, a rapid and robust constriction of smooth muscle cells restricts blood flow. Subsequently, changes in endothelial and smooth muscle cells promote complete closure of the lumen, a process that in humans takes one to three weeks. While much is known about the initial stage, less is understood about the molecular drivers associated with the later steps. Physiologically, it is understood that the initial constriction of the ductus arteriosus relies on increased arterial pO₂, decreased blood pressure in the DA lumen, reduction in circulating prostaglandin E₂ (PGE₂) and PGE₂ receptor levels. These events trigger rapid smooth muscle cell contraction through changes in intracellular calcium levels and a drastic reduction in PGE₂ signaling upon dissociation of the placenta which is the main source of PGE₂. Nonetheless, complete closure of the lumen requires the participation of the endothelium through relatively unknown mechanisms.

Here we sought to characterize the transcriptional changes involved in the closure of the ductus arteriosus by performing single cell RNAseq prior to, during and shortly after closure using the mouse as a model system. Using these data, our second goal was to identify novel regulators of developmentally programmed vascular remodeling. Here we communicate that vimentin, a type III intermediate filament is required for complete closure of the ductus arteriosus. Mechanistically we found that vimentin expression is needed to support the burst of Notch signaling associated with closure of this embryonic vessel. Reduction of Notch signaling affects both endothelial and smooth muscle cell remodeling ensuing incomplete shunting of the ductus arteriosus and resembling Jagged 1 inactivation (4,5).

MATERIALS AND METHODS

The authors declare that all supporting data, excluding that from scRNA-seq, are available within the article (and its online supplementary materials). All scRNA-Seq data are deposited on the international public repository Gene Expression Omnibus database (GEO) with accession number GSE188202.

Mice

For scRNA-seq experiments, C57BL/6J mice at the following stages were used: E18.5, P0.5 and P5. Libraries were generated from ducti of pooled littermates (8–9 mice per library, both sexes). Vimentin-deficient (*Vim*^{-/-}) mice were a gift from Albee Messing (Madison, WI); Jaglox/lox mice were a gift from Freddy Radke and have been previously used by our group (6,7). *Cdh5*-Cre were a generous gift from Ralph Adams (8).

Single-cell isolation

For cell isolation, aorta and ducti were dissected in versine; vessels were minced into small pieces and placed in 1mL of digestion buffer containing DNaseI, 1M HEPES, Liberase, and HBSS at 37C for 20mins. Once tissue was digested into a single cell suspension, cells were washed, pelleted, and passed through a 40µm filter. The final cell suspension was in 0.04%BSA.

Libraries for scRNA-seq were generated using 10X Genomics Chromium Single Cell 3' Library & Gel Bead Kit v3. Cells were loaded accordingly following the 10X Genomics protocol with an estimated targeted cell recovery of 6000 cells. Sequencing was performed on NovaSeq6000 (Pair-end, 100 base pairs per read). The digital expression matrix was generated by demultiplexing, barcode processing, and gene unique molecular index counting using the Cellranger count pipeline (version 4.0.0, 10X Genomics). Multiple samples were merged using the Cellranger aggr pipeline. To identify different cell types and find signature genes for each cell type, the R package Seurat (version 3.1.2) was used to analyze the digital expression matrix. Specifically, cells that express <100 genes or <500 transcripts were filtered out. The data were normalized using the NormalizeData function with a scale factor of 10,000. The genes were then scaled and centered using the ScaleData function. Principal component analysis (PCA), Uniform Manifold Approximation and Projection (UMAP) were used to reduce the dimensionality of the data. Cell clusters were identified using the FindClusters function. The cluster marker genes were found using the FindAllMarkers function. Cell types were annotated based on the cluster marker genes. Heatmaps, violin plots and gene expression plots were generated by DoHeatmap, VlnPlot, FeaturePlot functions, respectively. Data are available in the international public repository Gene Expression Omnibus database (GEO) under accession number GSE188202.

Immunofluorescence: For whole-mount aorta staining, mice were euthanized and perfused with 2% paraformaldehyde (PFA). The aortae were dissected from the backbone, cleaned, filleted open, and pinned down on silicone-coated plates with the endothelium facing up and left in 2% PFA overnight. The following day, aortae were washed three times in 1x PBS, blocked for 1hr, and primary antibodies were added in fresh blocking buffer overnight. On the second day the aortae were washed three times in 1x PBS and secondaries were added in fresh blocking buffer and allowed to incubate for 2 hrs followed by three washes. After the washes they were mounted onto slides using ProLong Gold Antifade Mounting Medium (Thermo Fischer Scientific P36930) covered with a coverslip and sealed with nail polish. The following primary antibodies and concentrations were used: Anti-Vimentin (Encor Biotech, # CPCA-Vim, 1:1000), anti-VE-cadherin goat polyclonal (Santa Cruz Biotechnology #sc-6458, 1:200), anti-ERG (ABCAM #ab92513, 1:200). PECAM clone 2H8 antibody was graciously provided by Dr. William Muller (Northwestern University, Chicago). The following secondary antibodies were used: Donkey anti-Rabbit Alexa Fluor™ 568 (Invitrogen A10042) used at 1:400; FITC-Donkey anti-Chicken (Thermo Fisher SA1-72000) used at 1:400; Donkey Anti-Goat Alexa Fluor® 647 (Abcam ab150135) used at 1:400; Alexa Fluor® 488 AffiniPure Goat Anti-Armenian Hamster (Jackson ImmunoResearch Laboratories 127-545-160) used at 1:400; and all

preparations were stained with DAPI (Thermo Fisher D1306) 1:500. Images were taken on a A1R HD25 confocal microscope (Nikon) using 20x, 40x and 60x objectives.

For histological sections: ducti arteriosus were dissected, fixed in 2% PFA overnight, washed 3 times in PBS and embedded first in Histogel under a dissecting microscope and later in paraffin. Blocks were sectioned at 5 μ M and stained with H&E by Northwestern Mouse Histology and Phenotyping Laboratory. Other sections were processed with the following primary antibodies: Anti-vimentin (Encor Biotech, # CPCA-Vim), Anti-Smooth Muscle alpha actin– Cy3 (C6198), Anti-smooth muscle Myosin heavy chain 11 (Abcam ab224804), Anti-Calponin 1 (Abcam ab46794), Anti-SM22 alpha (Abcam ab14106). The following secondary antibodies were used: Alexa-Fluor Donkey anti-Rabbit 568, FITC-Donkey anti-Chicken, and all preparations were also stained with DAPI (Thermo Fisher D1306).

Measurements of the ducti at several ages were done on an Echo Revolve microscope equipped with a micrometer for X and Y measurements. The ducti still attached to the dorsal aorta were carefully dissected and pinned onto silicone-coated dishes. Measurements were obtained always at the same distance from the aorta for accurate comparisons using 1.25X and 4X objectives.

Statistics: To quantify closure of the DA, a ratio of the outer width of the ductus arteriosus (DA) to the width of the descending aorta (AO) was calculated for each aorta at each time point, data were pooled from both male and female mice. Measurements were done on the Echo Revolve using the annotation tool, and statistics were performed on Graphpad Prism, not assuming normality in the data (data unpaired). The nonparametric Mann-Whitney test was performed for comparisons between Wild-type and Vimentin KO measurements at each developmental time point. A p-value of less than 0.05 was considered statistically significant.

RESULTS

Changes in Vimentin expression during the closure of the ductus arteriosus

Single-cell RNAseq (scRNA-seq) transcriptomics on the ductus arteriosus (DA) and aorta were conducted at developmental stages prior to constriction, at peak constriction, and at post-vessel occlusion (E18.5, P0.5, and P5; Figure 1A; Figure S1A, B, Table S1). Each DA was carefully dissected and enzymatically digested to generate 3 independent scRNA-seq libraries, without FACS-sorting (Figure 1A). Using dimensionality reduction by uniform manifold approximation and projection (UMAP), we identified 5 distinct cell types and assigned cellular identities based on canonical lineage markers (endothelial cells, vascular smooth muscle cells, fibroblasts, sympathetic nerve cells, and leukocytes) (Figure 1B-D, Figure S1C).

Analysis of differentially expressed genes in both endothelial and smooth muscle cells across the sharp temporal window of vascular remodeling uncovered interesting patterns with some genes peaking at E18.5, others at P0.5 and a last group at P5 (Figure 1D,E). Interestingly, evaluation of the top 30 differentially expressed genes showed a 53% overlap

between endothelial and smooth muscle cells. The common top 10 genes included two long non-coding RNAs (*Malat1* and *Tpt1*); four extracellular matrix transcripts (*Sparc*, *Colla2*, *Eln*, and *Mgp*) and three cytoskeletal proteins (*Vim*, *Tmsb4x* and *Actb*) (Figure 1F). The last of the gene cohort was eukaryotic translation elongation factor 1 alpha (*Eef1a1*) involved in modulation of cytoskeleton, and that also exhibits chaperone-like activity, controls proliferation and cell death. Interestingly, these transcripts exhibit a time-specific profile of upregulation being prior to, during, or after constriction.

Our particular interest when analyzing the data was to identify transcripts that sharply increased at P0.5, the most active period of DA closure, and that returned to steady-state or lower by P5. This profile was clearly followed by the intermediate filament Vimentin (*Vim*) (Figure 1F). Violin plots showed a bell-shaped curve with a peak at P0.5, a time of active DA remodeling and following the pattern that fulfilled our criteria.

Importantly, this bell-shape vimentin profile was shared by vascular endothelial, smooth muscle and fibroblast but not by leukocytes from the same scRNAseq libraries (Figure 2A). Additional immunocytochemical localization experiments showed protein accumulation in the endothelium and smooth muscle that decreased over time (P7 and 13 week adult DA) (Figure 2B). Absence of endothelial cells was clearly apparent by P7, as per lack of CD31. Remodeling of smooth muscle cells shown as clusters at the periphery of the DA 13 week remnant were also apparent (Figure 2B).

The potential contribution of vimentin in the closure of the ductus arteriosus has not been previously explored. We further considered vimentin as an interesting candidate to explore since intermediate filaments are well known to provide mechanical strain and resilience (9). Of note, vimentin's expression was unique amongst other intermediate filaments in the ductus arteriosus. Other members of the family, such as desmin and keratins were also expressed, but at lower levels and with patterns restricted to specific cell types; desmin in smooth muscle and keratins in endothelial cells (Figure 2C). Furthermore, neither desmin nor keratins showed an expression pattern that peaked at P0.5 and decrease thereafter, as displayed by vimentin.

To clarify whether the increased expression of *Vim* at P0.5 was specific to the DA instead of a general developmental pattern that extended to other vessels at equivalent age, we took advantage of scRNA-seq generated from aorta of the same mice where ducti was isolated (Figure 2D). Expression levels of *Vim* in the aortae were then used to normalize *Vim* transcripts of the DA to further assess levels per cell type and independent of global developmental patterns. These findings further confirmed sharp increases in *Vim* at P0.5 specifically in ducti endothelial cells, smooth muscle cells, and fibroblasts indicating that across these cell types, *Vim* expression raises sharply during the constriction of the DA at P0.5 (Figure 2E).

To directly test the potential contribution of vimentin in the closure of the DA, we took advantage of an established vimentin knock-out mouse model (*Vim*^{-/-}). Genomic deletion of vimentin was initially characterized by Colucci-Guyon in 1994 (10). *Vim*^{-/-} mice are viable and fertile. Evaluation of vimentin in the aortic endothelium confirmed the lack of

this type III intermediate filament in *Vim*^{-/-} mice with a contrasting robust expression noted in wild-type controls (Figure 3A). Transverse sections of adult dorsal aorta also showed high levels of vimentin in wild-type smooth muscle cells of the tunica media and its absence in null mice (Figure 3B).

The dynamics of DA closure were then traced in wild-type and *Vim*^{-/-} mice at time points ranging from P1 to 72 weeks of age (Figure 3C). Both groups showed striking and similar changes in the width of the DA with marked constrictions in the tunica media, indicating that the initial and robust contraction associated with changes in prostaglandin at birth was not affected by the absence of vimentin. Nonetheless, ducti of *Vim*^{-/-} mice frequently presented with visible internal blood suggesting the presence of a lumen. To rigorously quantify the process of closure, we evaluated 28 control mice and 31 *Vim*^{-/-} mice from P1 to 1 year of age (Figure 3D). Using external measurements, the data showed differences only in adult mice, where the diameter of the ductus failed to undergo complete remodeling in mice deleted for *Vim*. Consistent with the presence of a continuous lumen, *en face* evaluation of the aorta of adult *Vim*^{-/-} mice revealed the retention of an ostium in the area associated with the connection to the ductus arteriosus (Figure 3E) in all mice evaluated.

Macroscopic evaluation rendered wild-type and *Vim*^{-/-} mice similar, except for the presence of blood cells in the DA of *Vim*^{-/-} mice at both early and late stages; indicating the retention of an open communication between the pulmonary artery and the aorta. Using presence of blood in the DA as a read-out for patency, we found that all adult *Vim*^{-/-} mice evaluated had incomplete closure (Figure 3F). This was further confirmed by examination of cross-sections from *Vim*^{-/-} DA at 52w of age (Figure 3G) and was consistent with the openings noted in the lateral aspects of the adult aorta of *Vim*^{-/-}, where these ducti connect (Figure 3E). Additional histological evaluations of ducti from control and *Vim*^{-/-} mice confirmed clear retention of patency and absence of full cellular remodeling (Figure 3G). Progressive temporal evaluations of DA revealed that defects in *Vim*^{-/-} mice involve both the endothelium and the smooth muscle cell compartments. Specifically, by P3 the lumen of the DA in *Vim*^{-/-} mice is more obviously enlarged than in the wild-type littermates and DA patency is clearly retained in *Vim*^{-/-} adult mice (13weeks) (Figure 4A). Early remodeling of smooth muscle cells was also impaired with reduced number of *Vim*^{-/-} cells reorienting at P3 under the tunica intima (Figure 4A). Later remodeling was also affected as the fibrotic transition and peripheral clusters of smooth muscle cells apparent in wild-type at 13weeks were absent from *Vim*^{-/-} ducti of the same age (Figure 4A). In fact, ducti from *Vim*^{-/-} adult mice (13weeks) displayed an arrest in the progression of cellular remodeling. Specifically, *Vim*^{-/-} ducti had persistence of patency, incomplete reorientation of smooth muscle cells and absence of fibrosis at 13 weeks (Figure 4A). Combined these findings support the conclusion that vimentin is required not for the initial constriction of the ductus, but for the cellular remodeling that follows. This second phase of endothelial and smooth muscle cell remodeling is necessary for the complete obliteration of the vascular lumen. Next, we were naturally intrigued about potential underlying mechanisms and evaluation of the literature revealed links between vimentin and Notch (11,12).

It is well-accepted that signaling between endothelial cells and vascular smooth muscle cells through the Notch pathway contributes to arterial remodeling. Additionally, it has been

demonstrated that the absence of the Notch receptor Jagged1 in smooth muscle cells, results in patent ductus arteriosus (4). Interestingly, vimentin plays an important role in Notch transactivation (11). Specifically, depletion of vimentin reduces Jagged1-Notch signaling due to alterations in cellular stiffness which likely impair the pulling Jagged1—Notch force that precedes ADAM cleavage. Therefore, we first explored expression patterns of Notch signaling in the ductus arteriosus. Interestingly, we found that Jag1 expression in endothelial and vascular smooth muscle cells increased at P0.5, coincident with Vimentin upregulation during DA remodeling (Figure 4B). Therefore, the concurrent expression and raise of vimentin and Jag1 transcripts lends to the hypothesis that PDA in *Vim*^{-/-} mice might emerge from ineffective signaling between Jag1 (in endothelial cells) and Notch (in smooth muscle cells). Importantly, PDA have been reported upon inactivation of Jag1, as well as combined inactivation of Notch2 and 3 (4, 5,13).

To compare the phenotypes of Jagged1 deletion to that of *Vim*^{-/-} mice, we evaluated ducti from Jag1^{ECKO/SMKO} (Figure 4C). In fact, inactivation of vimentin phenocopies deletion of Jag1 in vascular cells. Cre-negative littermates showed closed lumen by P1 and presence of Jagged1 in the endothelium and in smooth muscle cells, albeit more reduced in this second cell type. In contrast, inactivation of Jagged1 in Cre-positive littermates was associated with clear lumens filled with red blood cells (Figure 4C).

Next, we sought to determine whether absence of vimentin affected Notch signaling. While overall levels of Notch3 were equally high in control littermates and vimentin null mice, the presence of Notch3 in the nucleus was only observed in smooth muscle cells from control mice being absent from *Vim*^{-/-} mice. This finding was obvious at P1 (Figure 5A) a time of active DA remodeling and also apparent at P3 (Figure 5B). Importantly, we also documented excess of endothelial cell proliferation in the endothelium of *Vim*^{-/-} mice at P1 and P3 (Figure S2A, B). This phenotype is also consistent with loss or reduced Notch signaling and likely underlies the reorganization of the lumen by P3 (Figure S2B)

The findings indicate that vimentin is required for appropriate Notch signaling strength and nuclear translocation. In the absence of vimentin, Notch signaling is impaired resulting in the arrest of cellular remodeling and retention of a functional lumen in the ductus arteriosus.

DISCUSSION

Resolution of individual transcriptional changes at the cellular level offers an unprecedented opportunity to seek answers to questions that require complex developmental events. In the case of the remodeling of the ductus arteriosus, scRNAseq revealed a large number of transcriptional alterations in the endothelial, smooth muscle and fibroblast compartments which will likely offer opportunities for exploration by multiple laboratories.

Seeking transcripts that sharply increase in the aorta shortly after birth, we identified vimentin, an intermediate filament protein highly expressed in both endothelial and smooth muscle cells. Interestingly, while viable and fertile (10), we found that mice with genomic deletion of vimentin exhibit incomplete closure of the ductus arteriosus due to failure in vascular remodeling. In fact, our data show that *Vim*^{-/-} mice at 1 year of age, still exhibit

an open lumen with visible presence of blood. Temporal evaluation of ducti from P0.5 to adulthood revealed defects in vascular remodeling that affect both the endothelial and smooth muscle cell compartments (Figure 5C). Specifically, we found excessive endothelial cell proliferation with retention of a lumen by P3 which did not change overtime. We also noticed alterations in smooth muscle cell remodeling with incomplete re-orientation of smooth muscle cells and lack of transition to a fibroblastic phenotype. In fact, retention of smooth muscle cell markers in the layers proximal to the endothelium.

Intermediate filaments cooperate with other elements of the cytoskeleton to provide structural support and mechanical integration between the cell surface, organelles and the nucleus (9,14,15). However, intermediate filaments distinguish themselves from other members of the cytoskeleton by their higher mechanical integrity and resistance to rupture (14,16). This is particularly important for cells that either withstand and/or impose physical forces, such as those occurring during vascular remodeling. While other types of intermediate filaments are expressed by smooth muscle (e.g., desmin) and by endothelial cells (e.g., keratins 8 and 18), the levels of vimentin supersede those in both cell types. Furthermore, in addition to their roles in maintaining mechanical integrity, vimentin undergoes impressive spatial rearrangement in smooth muscle cells during contraction and upon stimulation by several agonists (17,18). Importantly, vimentin has been implicated in the distribution of Ca^{2+} /calmodulin-dependent protein kinase II (CamKII), a kinase critical in regulating smooth muscle cell contraction (19). In endothelial cells, vimentin has been implicated in barrier function and cell adhesion (20), but no studies have explored the potential role of vimentin during vascular remodeling.

The process of complete closure of the DA is known to require smooth muscle cell migration and proliferation, disruption of the internal elastic lamina, alterations in extracellular matrix production, endothelial cell proliferation and monocyte adhesion (2–4,21–27). Many of these events require Notch signaling, particularly those associated with smooth muscle cell contraction (4,11). Recently, vimentin was shown to contribute to the mechanochemical transduction pathway that regulates multilayer cross-talk and structural homeostasis through the Notch signaling pathway (11). Consistent with those findings, here we showed that nuclear translocation of the intracellular domain of Notch3, the hallmark of Notch signaling, is impaired in the absence of vimentin. How can vimentin affect Notch signaling? It is well known that activation of Notch signaling requires a mechanical pulling force that is depending on the cytoskeleton (28). While only the actin has been implicated, recently published associations between actin and vimentin have been identified, uncovering an important continuum of interconnected cytoskeletal proteins particularly at the cell cortex (29). Therefore, low stiffness associated with lack of vimentin (30,31) is consistent with deficiencies in force generation needed for Notch signaling. In this context it is also important to emphasize that lack of vimentin is not equivalent to complete absence of Notch signaling. Absence of vimentin only impairs robust Notch signaling which is absolutely required for complete closure of the ductus arteriosus. In fact, patent ductus arteriosus occurs upon inactivation of Jagged1 in endothelial and smooth muscle cells and in compound Notch 2 and 3 genomic inactivation (4, 5, 13).

Given the fact that absence of vimentin is compatible with life and that mice reach adulthood, an obvious question is whether the mice develop signs of heart failure or pulmonary hypertension. In fact, no obvious abnormalities in the heart or lung were noted. This is likely due to the relatively narrow lumen that is retained in vimentin null mice. Our findings indicate that the initial stages that trigger the closure of the DA, namely the drastic contraction driven by prostaglandin at birth (32) is not compromised by the absence of vimentin. Instead, it is the subsequent steps associated with endothelial and smooth muscle cell remodeling the ones affected by vimentin deletion. Changes in orientation of smooth muscle cells and elimination of endothelial cells require vimentin and robust Notch signaling. Furthermore, whether PDA patients develop heart failure depends not only on the decrease in pulmonary vascular resistance but also on the ability of the left ventricle to handle the increase in volume overload (33). Thus, it is the size of the PDA and the relative blood volume that traffics through this vessel, that correlate with more severe clinical presentations and in fact, small lumen PDAs can be found in adult patients with little clinical manifestations (34).

Little is known about the cellular and molecular processes associated with the complete closure of a vascular lumen, the last step in DA remodeling. Our findings highlight the exquisite requirement of vimentin for the completion of this process in the ductus arteriosus.

Supplementary Material

Refer to Web version on PubMed Central for supplementary material.

ACKNOWLEDGEMENTS

We would like to thank the Jonsson Comprehensive Center at UCLA for sequencing of scRNAseq libraries and the Mouse Histology and Phenotyping core at Northwestern University. A special thanks to Michelle Steel and Snezana Mirkov for support with animal colonies, assistance with husbandry and mouse experimentation.

SOURCES OF FUNDING

This work was supported by R35HL140014 to M.L. Iruela-Arispe, Howard Hughes Medical Institute Gilliam Fellowship (GT11560) to Gloria Hernandez. Northwestern University Molecular and Translational Cardiovascular Training Program (T32HL134633; SP0040691) to Jocelynda Salvador. R Goldman and K Ridge are supported by NIGMS PO1 GM096971. R Goldman is supported by NIGMS PO1 GM096971. Karen Ridge is supported by NIGMS PO1 GM096971 and NHLBI P01HL154998.

NONSTANDARD ABBREVIATIONS AND ACROYNMS

DA	Ductus Arteriosus
PDA	Patent Ductus Arteriosus
AO	Aorta
scRNA-seq	single-cell RNA-sequencing
UMAP	uniform manifold approximation and projection
Vim	Vimentin

REFERENCES

1. Schneider DJ, Moore JW. Patent ductus arteriosus. *Circulation*. 2006; 114:1873–1882. [PubMed: 17060397]
2. Hsu H-W, Lin T-Y, Liu Y-C, Yeh J-L, Hsu J-H. Molecular Mechanisms Underlying Remodeling of Ductus Arteriosus: Looking beyond the Prostaglandin Pathway. *Int J Mol Sci*. 2021; 22:3238 [PubMed: 33810164]
3. Hung Y-C, Yeh J-L, Hsu J-H. Molecular mechanisms for regulating postnatal ductus arteriosus closure. *Int J Mol Sci*. 2018; 19:1861. [PubMed: 29941785]
4. Feng X, Krebs LT, Gridley T. Patent ductus arteriosus in mice with smooth muscle-specific Jag1 deletion. *Development*. 2010; 137:4191–4199. [PubMed: 21068062]
5. Krebs LT, Norton CR, Gridley T. Notch signal reception is required in vascular smooth muscle cells for ductus arteriosus closure. *Genesis*. 2016; 54:86–90. [PubMed: 26742650]
6. Hofmann JJ, Zovein AC, Koh H, Radtke F, Weinmaster G, Iruela-Arispe ML. Jagged1 in the portal vein mesenchyme regulates intrahepatic bile duct development: insights into Alagille syndrome. *Development*. 2010; 137:4061–4072.
7. Hofmann JJ, Briot A, Enciso J, Zovein AC, Ren S, Zhang ZW, Radtke F, Simons M, Wang Y, Iruela-Arispe ML. Endothelial deletion of murine Jag1 leads to valve calcification and congenital heart defects associated with Alagille syndrome. *Development*. 2012; 139:4449–4460. [PubMed: 23095891]
8. Wang Y, Nakayama M, Pitulescu M, et al. Ephrin-B2 controls VEGF-induced angiogenesis and lymphangiogenesis. *Nature*. 2010; 465:483–486. [PubMed: 20445537]
9. Patteson AE, Vahabikashi A, Pogoda K, Adam SA, Mandal K, Kittisopikul M, et al. Vimentin protects cells against nuclear rupture and DNA damage during migration. *J Cell Biol*. 2019; 218:4079–4092. [PubMed: 31676718]
10. Colucci-Guyon E, Portier MM, Dunia I, Paulin D, Pournin S, Babinet C. Mice lacking vimentin develop and reproduce without an obvious phenotype. *Cell*. 1994; 79:679–694. [PubMed: 7954832]
11. van Engeland NCA, Suarez Rodriguez F, Rivero-Müller A, Ristori T, Duran CL, Stassen OMJA, et al. Vimentin regulates Notch signaling strength and arterial remodeling in response to hemodynamic stress. *Sci Rep*. 2019; 9:12415. [PubMed: 31455807]
12. Antfolk D, Sjöqvist M, Cheng F et al. Selective regulation of Notch ligands during angiogenesis is mediated by vimentin. *Proc Natl Acad Sci USA*. 2017; 114:E4574–E4581. [PubMed: 28533359]
13. Baeten JT, Jackson AR, McHugh KM, Lilly B. Loss of Notch2 and Notch3 in vascular smooth muscle causes patent ductus arteriosus. *Genesis*. 2015; 53:738–748. [PubMed: 26453897]
14. Chang L, Goldman RD. Intermediate filaments mediate cytoskeletal crosstalk. *Nat Rev Mol Cell Biol*. 2004; 5:601–613. [PubMed: 15366704]
15. Lowery J, Kuczumski ER, Herrmann H, Goldman RD. Intermediate filaments play a pivotal role in regulating cell architecture and function. *J Biol Chem*. 2015; 290:17145–17153. [PubMed: 25957409]
16. Köster S, Weitz DA, Goldman RD, Aebi U, Herrmann H. Intermediate filament mechanics in vitro and in the cell: from coiled coils to filaments, fibers and networks. *Curr Opin Cell Biol*. 2015; 32:82–91. [PubMed: 25621895]
17. Li Q-F, Spinelli AM, Wang R, Anfinogenova Y, Singer HA, Tang DD. Critical role of vimentin phosphorylation at Ser-56 by p21-activated kinase in vimentin cytoskeleton signaling. *J Biol Chem*. 2006; 281:34716–34724. [PubMed: 16990256]
18. Tang DD, Bai Y, Gunst SJ. Silencing of p21-activated kinase attenuates vimentin phosphorylation on Ser-56 and reorientation of the vimentin network during stimulation of smooth muscle cells by 5-hydroxytryptamine. *Biochem J*. 2005; 388:773–783. [PubMed: 15766329]
19. Marganski WA, Gangopadhyay SS, Je H-D, Gallant C, Morgan KG. Targeting of a novel Ca²⁺/calmodulin-dependent protein kinase II is essential for extracellular signal-regulated kinase-mediated signaling in differentiated smooth muscle cells. *Circ Res*. 2005; 97:541–549. [PubMed: 16109919]

20. Dave JM, Bayless KJ. Vimentin as an integral regulator of cell adhesion and endothelial sprouting. *Microcirculation*. 2014; 21:333–344. [PubMed: 24387004]
21. Mueller PP, Drynda A, Goltz D, Hoehn R, Hauser H, Peuster M. Common signatures for gene expression in postnatal patients with patent arterial ducts and stented arteries. *Cardiol Young*. 2009; 19:352–359. [PubMed: 19538825]
22. Hsieh Y-T, Liu NM, Ohmori E, et al. Transcription profiles of the ductus arteriosus in Brown-Norway rats with irregular elastic fiber formation. *Circ J*. 2014; 78:1224–1233. [PubMed: 24647370]
23. Shelton EL, Ector G, Galindo CL, et al. Transcriptional profiling reveals ductus arteriosus-specific genes that regulate vascular tone. *Physiol Genomics*. 2014; 46:457–466. [PubMed: 24790087]
24. Goyal R, Goyal D, Longo LD, Clyman RI. Microarray gene expression analysis in ovine ductus arteriosus during fetal development and birth transition. *Pediatr Res*. 2016; 80:610–618. [PubMed: 27356085]
25. Liu NM, Yokota T, Maekawa S, et al. Transcription profiles of endothelial cells in the rat ductus arteriosus during a perinatal period. *PLoS One*. 2013; 8:e73685. [PubMed: 24086288]
26. Saito J, Kojima T, Tanifuji S, et al. Transcriptome Analysis Reveals Differential Gene Expression between the Closing Ductus Arteriosus and the Patent Ductus Arteriosus in Humans. *J Cardiovasc Dev Dis*. 2021; 8:45. [PubMed: 33923468]
27. Bökenkamp R, Raz V, Venema A, et al. Differential temporal and spatial progerin expression during closure of the ductus arteriosus in neonates. *PLoS One*. 2011; 6:e23975. [PubMed: 21915271]
28. Meloty-Kapella L, Shergill B, Kuon J, Botvinick E, Weinmaster G. Notch ligand endocytosis generates mechanical pulling force dependent on dynamin, epsins, and actin. *Dev Cell*. 2012; 22:1299–1312. [PubMed: 22658936]
29. Wu H, Shen Y, Sivagurunathan S, Weber MS, Adam SA, Shin JH, Fredberg JJ, Medalia O, Goldman R, Weitz DA. Vimentin intermediate filaments and filamentous actin form unexpected interpenetrating networks that redefine the cell cortex. *Proc Natl Acad Sci U S A*. 2022; 119:e2115217119. [PubMed: 35235449]
30. Gladilin E, Gonzalez P, Eils R. Dissecting the contribution of actin and vimentin intermediate filaments to mechanical phenotype of suspended cells using high-throughput deformability measurements and computational modeling. *J Biomech*. 2014; 47:2598–2605. [PubMed: 24952458]
31. Guo M, Ehrlicher AJ, Mahammad S, Fabich H, Jensen MH, Moore JR, Fredberg JJ, Goldman RD, Weitz DA. The role of vimentin intermediate filaments in cortical and cytoplasmic mechanics. *Biophys J*. 2013; 105:1562–1568. [PubMed: 24094397]
32. Nguyen M, Camenisch T, Snouwaert JN, Hicks E, Coffman TM, Anderson PA, Malouf NN, Koller BH. The prostaglandin receptor EP4 triggers remodelling of the cardiovascular system at birth. *Nature*. 1997; 390:78–81. [PubMed: 9363893]
33. Rudolph AM. *Congenital Diseases of the Heart: Clinical-physiologic Considerations*. 3rd ed. San Francisco: Wiley-Blackwell. 2009.
34. Ng AS, Vlietstra RE, Danielson GK, Smith HC, Puga FJ. Patent ductus arteriosus in patients more than 50 years old. *Int J Cardiol*. 1986; 11:277–285. [PubMed: 3721629]

HIGHLIGHTS

- Single-cell RNA-sequencing on the ductus arteriosus at E18.5, P0.5, and P5 reveals how the ductus arteriosus undergoes drastic transcriptional changes at the single-cell level.
- Endothelial cells increase levels of Vimentin transcripts soon after birth (P0.5), concurrent with ductus arteriosus closure.
- Loss of vimentin, the major intermediate filament protein of endothelial cells, prevents proper permanent closure of the ductus arteriosus.
- Absence of vimentin impairs Notch signaling in the ductus arteriosus and the phenotype resembles Jag1 EC/SMC inactivation

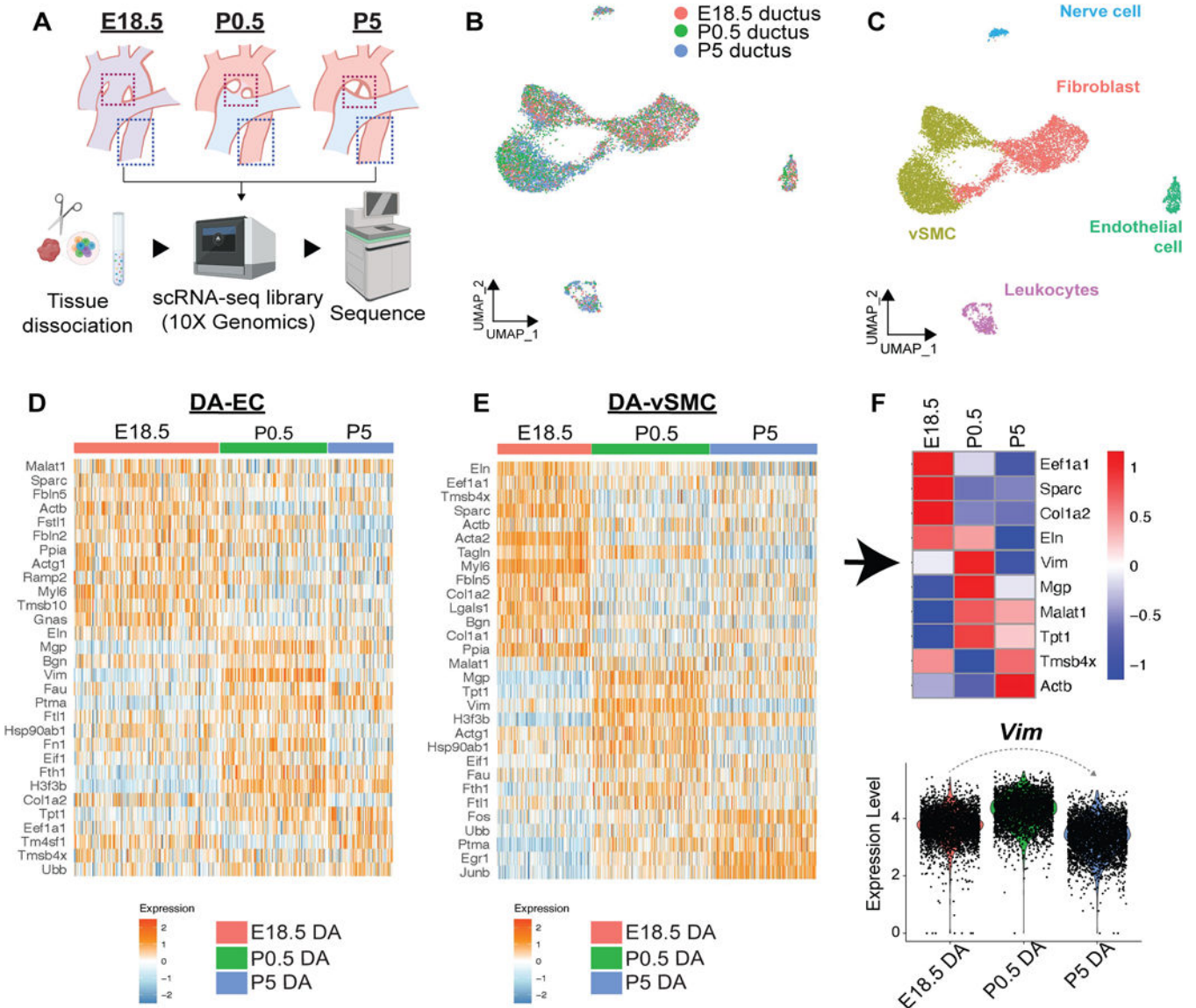


Figure 1. scRNA-Seq identifies vimentin expression peaking during DA closure

A. Schematic illustrating the isolation of ductus arteriosus (magenta dotted line) and aortic (blue dotted line) cells for single-cell RNA sequencing.

B. Uniform manifold approximation and projection (UMAP) plot of cells from three independent libraries: E18.5, P0.5, and P5 ductus arteriosus. 8–9 ductus arteriosus (ductus, DA) were used per library.

C. UMAP analysis and heat map-style representation of canonical lineage markers.

D. Heat map of the top 30 genes in the ductus arteriosus – endothelial compartment (DA-EC).

E. Heat map of the top 30 genes in the ductus arteriosus – vascular smooth muscle cell compartment (DA-vSMA).

F. Top: heat map of the top 10 genes in each ductus arteriosus library at the respective time points (E18.5, P0.5 and P5). Arrow identifies vimentin (*Vim*) as the transcript that shows

Author Manuscript

Author Manuscript

Author Manuscript

Author Manuscript

the highest expression at P0.5 with drastic drop at P5. Bottom: graph illustrating bell-shape expression pattern of vimentin.

Author Manuscript

Author Manuscript

Author Manuscript

Author Manuscript

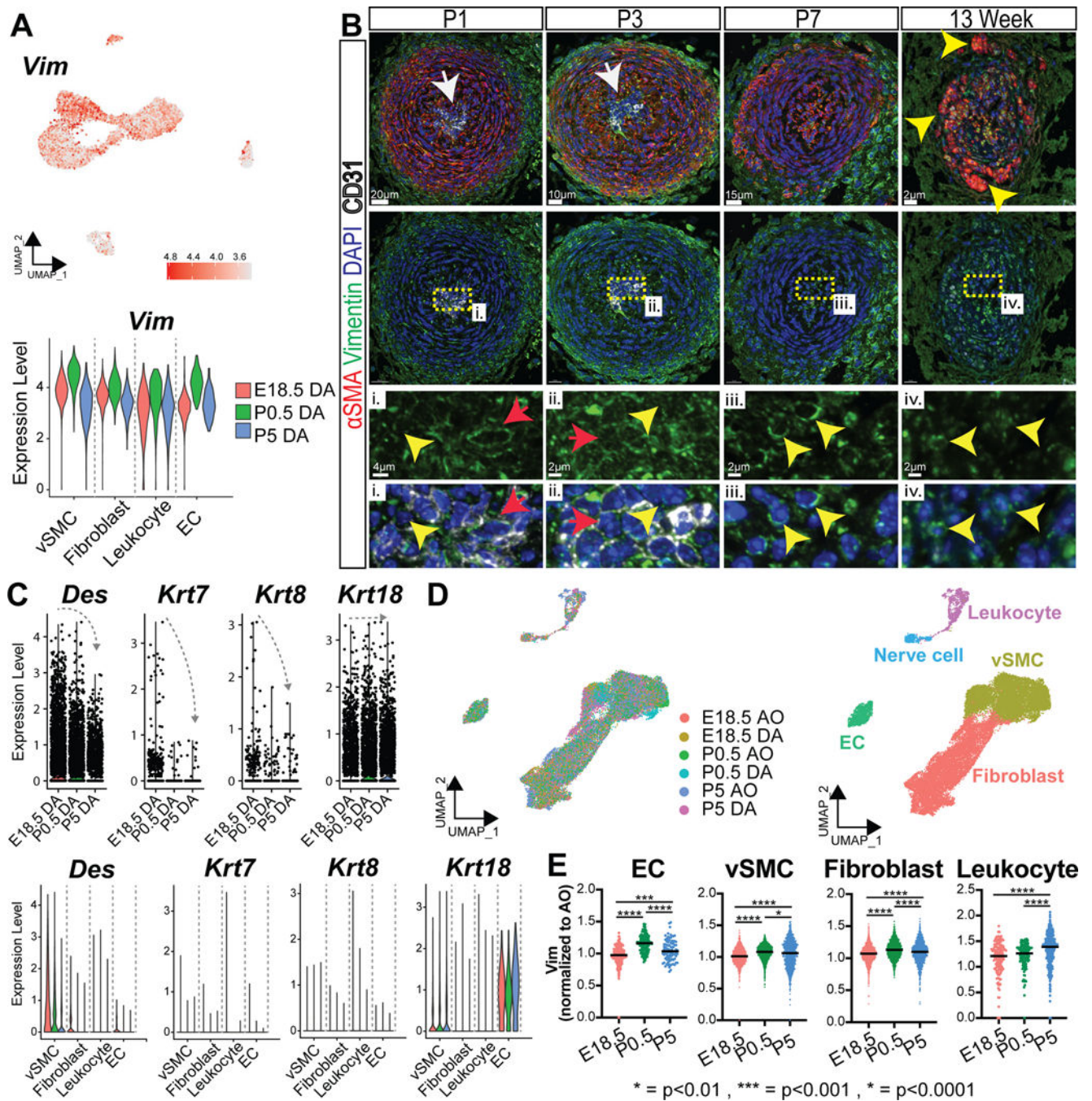


Figure 2: Vimentin expression and cellular localization during the closure of the ductus arteriosus

A. Left: UMAP representation of Vimentin (*Vim*) expression. Bottom: *Vim* expression levels in each cell type at the indicated time-points.

B. Vimentin staining in cross-sections of DA at P1, P3, P7 and 13-week old WT mice. White arrows indicate CD31+ ECs in the constricting lumen at P1 and P3. By P7, the lumen is permanently closed and SMCs remodel into peripheral clusters by 13 weeks (yellow

arrows). Magnification of the central lumen regions (i.-iv.) indicate expression of vimentin in both ECs (red arrows) and SMCs (yellow arrowheads).

C. Violin plots show overall expression of intermediate filaments in the ductus arteriosus at each given time point as normalized gene expression per cell. Dotted grey arrows note expression trends through time. Also shown on the bottom, intermediate filament expression in the ductus arteriosus at each time point per cell type.

D. UMAP plot of cells from 6 libraries: the DA and aorta (AO) at E18.5, P0.5, and P5, isolated from the same mice (schema in Figure 1A) and cellular identities assigned to each cluster on the right UMAP.

E. Normalized DA vimentin expression to aortic vimentin expression from each cell type at the indicated time points.

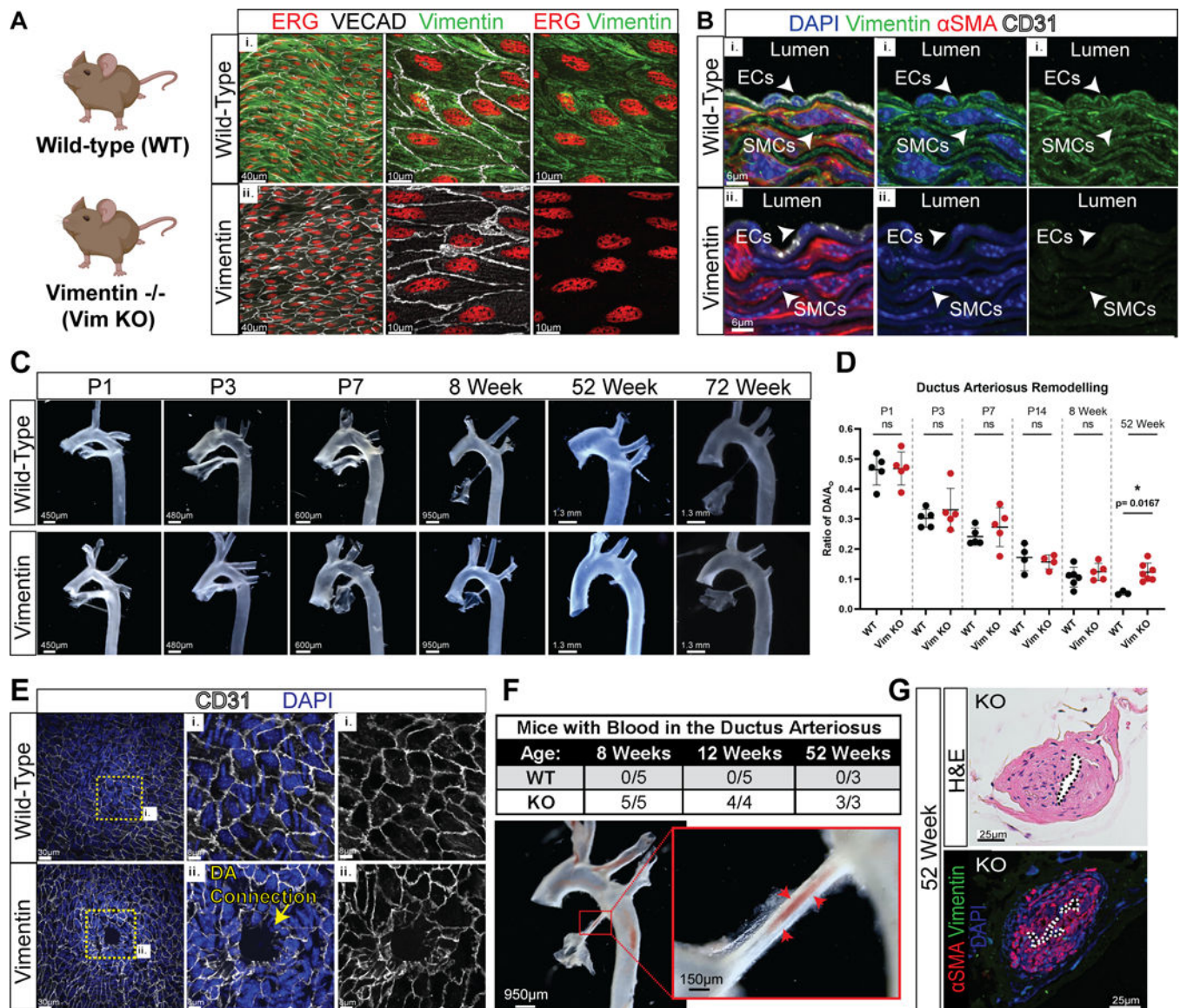


Figure 3: Vimentin null mice are viable but exhibit patent ductus arteriosus

A: *En face* immunofluorescence preparation of aortae confirming presence and absence of vimentin in the endothelium of the wild-type (WT) (i) and knock-out (*Vim*^{-/-}) mice (ii), respectively. Vimentin in green; ERG, a nuclear endothelial transcription factor in red; VE-Cadherin in white.

B. Transversal sections of the descending aorta at P7 from WT and *Vim*^{-/-} mice demonstrate the abundance of vimentin (arrowheads) in endothelial cells (ECs) (white) and smooth muscle cells (SMCs) (red) in the intimal and medial layers of the aorta, respectively.

C. Dark field imaging of aortae at different developmental timepoints highlights the relationship of the aorta to the ductus arteriosus in wild-type and *Vim*^{-/-} mice from P1 to 72 weeks of age.

D. Quantification of the width of the ductus arteriosus (DA) normalized to the width of the descending aorta (AO). (n=6 per group, p=0.0167).

E. *En face* staining of the aortic endothelium in the region of the ductus arteriosus opening along the aorta in 20 week old WT and *Vim*^{-/-} mice. Note, *Vim*^{-/-} showed opening into the ductus arteriosus (ii). CD31 in white, DAPI in blue. The image is representative of n=5 adult animals evaluated.

F. Quantification of proportion of adult mice (8weeks-52weeks) with blood in the ductus arteriosus. n=3-5 mice per time point.

G. Transversal sections of the DA from 52 week *Vim*^{-/-} mice stained with H&E and stained for alpha smooth muscle alpha actin (red), vimentin (green) and DAPI (blue). Despite absence of observable differences in outer widths of the vessel in **2D & 2E** the lumen is retained and SMCs still retain smooth muscle cell markers.

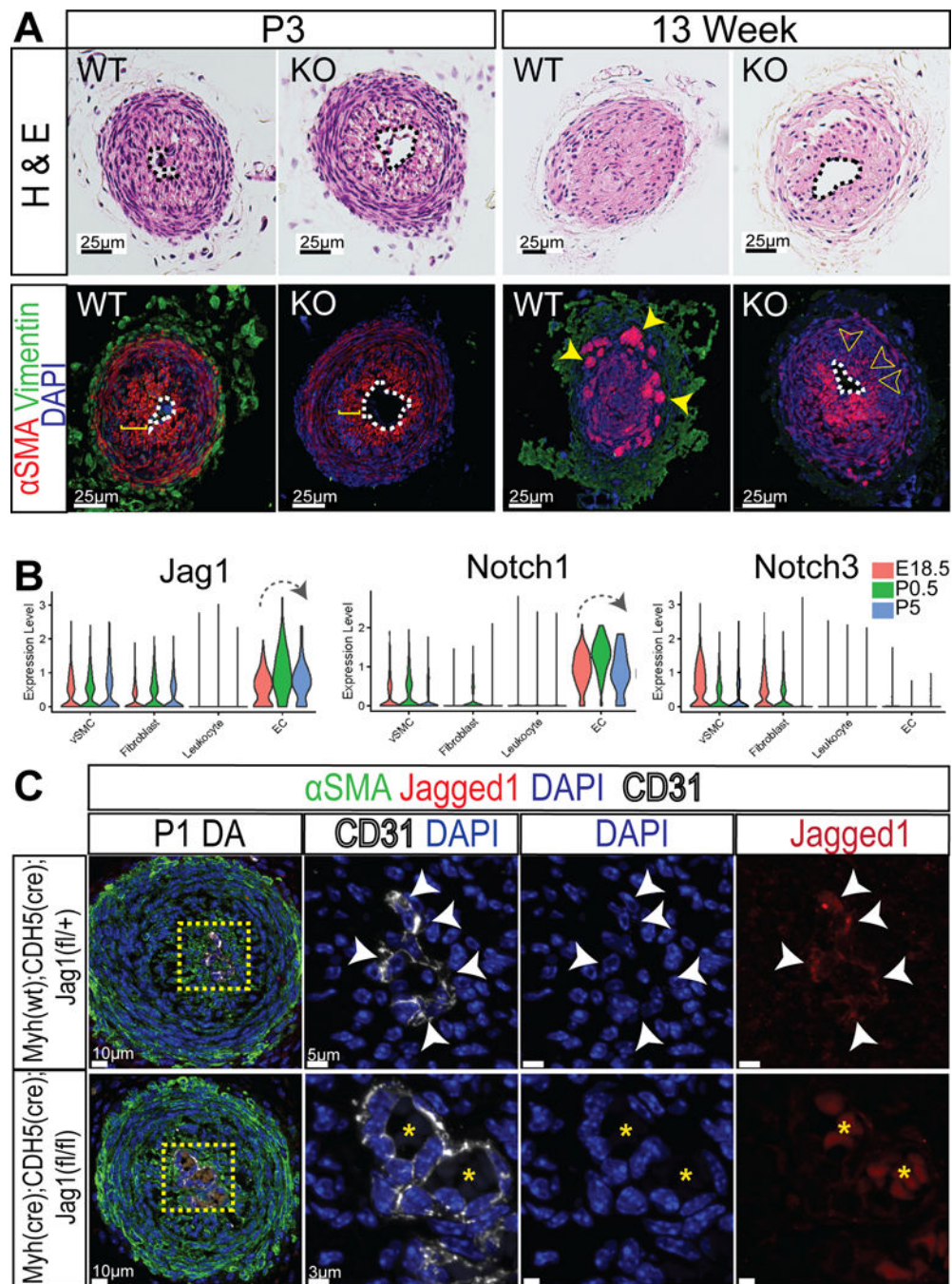


Figure 4: Cellular remodeling defects in *Vim*^{-/-} mice phenocopies defects in Notch signaling
A. Transverse sections of the ductus arteriosus in WT and *Vim*^{-/-} mice at P3 and 13 weeks of age stained for vimentin (green) and the smooth muscle marker, alpha-SMA (red). Note clear retention of lumen at 13 weeks in *Vim*^{-/-} in contrast to controls. Also note drastic remodeling of smooth muscle (clusters) WT mice (filled yellow arrowheads) not detected in *Vim*^{-/-} mice. Also, note incomplete circular reorientation of smooth muscle cells (open arrowheads) in *Vim*^{-/-} mice

B. Violin plots showing overall expression of *Jag1*, *Notch1*, and *Notch3* in the ductus arteriosus at each given timepoint shown as normalized gene expression per cell. Dotted grey arrows note expression trends through time.

C. Cross sections of ducti from P1 *Jag1* control (top row) and *Jag1*^{ECKO/SMKO} (bottom row) confirmed published studies describing patent ductus arteriosus in *Jag1*^{SMKO} mice and demonstrate the resemblance to *Vim*^{-/-} mice. In control mice: lumen is constricted and ECs (white) are positive for *Jag1*, ligand for Notch. In contrast, *Jag1*^{ECKO/SMKO} ducti have a clear open lumen and are *Jag1* negative (red autofluorescence is from blood cells present in the open lumen).

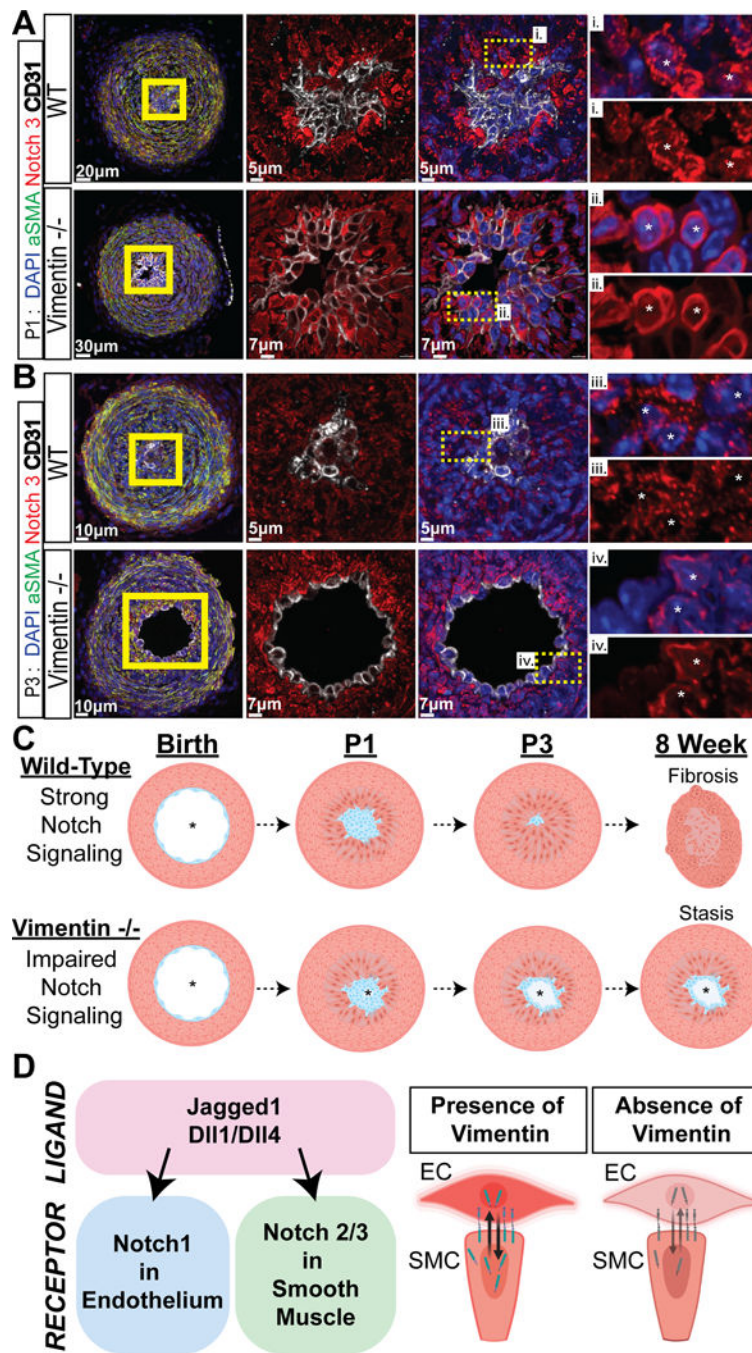


Figure 5: Vimentin knockout mice have impaired Notch3 signaling

A. Cross-sections of P1 WT and Vim KO ducts stained for Notch3 (red), α -SMA (green) and CD31 (white). Wild-type SMCs adjacent to ECs display cytoplasmic and nuclear Notch3 staining (i.), while Vim KO SMCs staining for Notch3 is restricted to the cytoplasmic region (ii.). Note the open lumen in Vim KO DA.

B. Cross-sections of P3 WT and Vim KO ducts stained for Notch3 (red), α -SMA (green) and CD31 (white). Wild-type SMCs adjacent to ECs display cytoplasmic and nuclear Notch3 staining (i.), while Vim KO SMCs staining for Notch3 is restricted to the

cytoplasmic region (ii.). Note the lack of EC-SMC remodeling leading to permanent DA closure by P3.

C. Schematic depicting the findings of this study. Following initial constriction mediated by prostaglandin, wild-type ducti with strong Notch signaling undergoes endothelial and smooth muscle cell remodeling completing the closure of the DA and leading to fibrosis by 8 weeks. In contrast, absence of vimentin leads to impaired Notch signaling and incomplete remodeling of the DA that retains an open lumen.

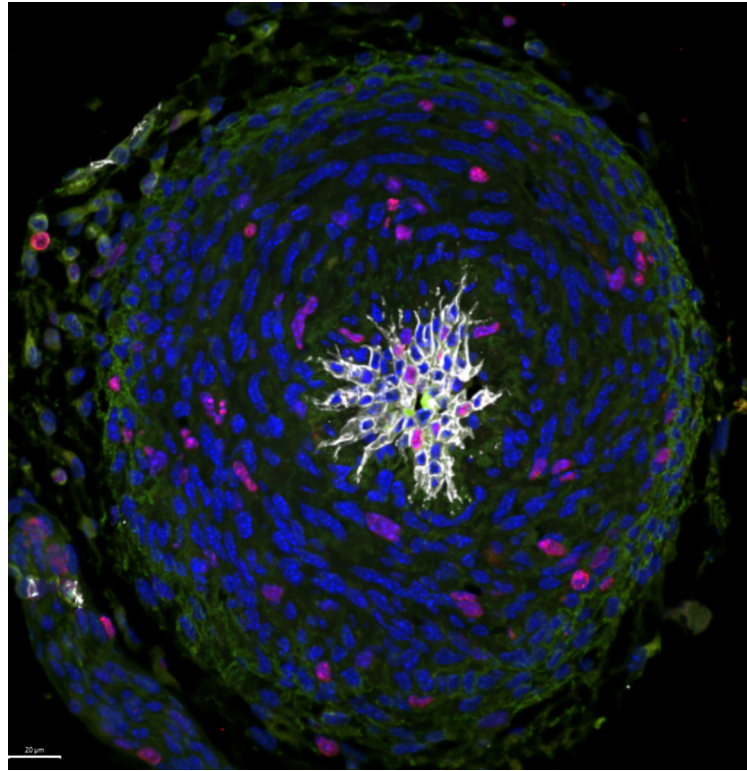
D. Schematic of the proposed mechanism of normal and altered Notch signaling between EC-SMCs in WT and Vim KO ducti. Jagged1 and Dll1/Dll4 are ligands for Notch1 in ECs and Notch3 in SMCs. Absence of vimentin reduces cell stiffness which affects the force necessary for Notch activation (cleavage).

Author Manuscript

Author Manuscript

Author Manuscript

Author Manuscript



Author Manuscript

Author Manuscript

Author Manuscript

Author Manuscript